Navigating the Hilbert space of nonseparable elastic states in arrays of periodically coupled one-dimensional waveguides

P. A. Deymier (iD), M. A. Hasan (iD), and K. Runge (iD)

COLLECTIONS

View Online

Export Citation

CrossMark

Navigating the Hilbert space of nonseparable elastic states in arrays of periodically coupled one-dimensional waveguides

View Online   Export Citation   CrossMark

P. A. Deymier,[a] [iD] M. A. Hasan,[b] [iD] and K. Runge[b] [iD]

AFFILIATIONS

Department of Materials Science and Engineering, University of Arizona, Tucson, Arizona 85721, USA

[a]Author to whom correspondence should be addressed: deymier@email.arizona.edu and deymier@arizona.edu
[b]Electronic addresses: mdhasan@arizona.edu and krunge@arizona.edu

ABSTRACT

A planar array of three one-dimensional elastic waveguides mutually coupled periodically along their length and driven externally is shown theoretically and numerically to support nonseparable superpositions of states. These states are the product of Bloch waves describing the elastic displacement along the waveguides and spatial modes representing the displacement across the array of waveguides. For a system composed of finite length waveguides, the frequency, relative amplitude, and phase of the external drivers can be employed to selectively excite specific groups of discrete product modes. The periodicity of the coupling is used to fold bands enabling superpositions of states that span the complete Hilbert space of product states. We show that we can realize a transformation from one type of nonseparable superposition to another one that is analogous to a nontrivial quantum gate. This transformation is also interpreted as the complex conjugation operator in the space of the complex amplitudes of individual waveguides.

I. INTRODUCTION

Superposition of states and entanglement are at the core of today's second quantum revolution.[1] Entangled superpositions of states possess two distinct attributes, namely, nonlocality and nonseparability. Nonlocality is a unique feature of quantum mechanics, but nonseparability is not. The notion of "classical entanglement," i.e., local nonseparable superposition of states, has received a significant amount of attention, theoretically and experimentally, in the area of optics.[2–8] However, to date, much less attention has been paid to other classical waves such as elastic waves; yet, remarkable new behaviors of sound, analogous to quantum physics, such as the notions of elastic pseudospin[9–19] and Zak/Berry phase,[20–28] are emerging. Recently, elastic nonseparable states,[29] analogous to "classically entangled" states, were observed in externally driven systems composed of parallel arrays of one-dimensional elastic waveguides coupled elastically and uniformly along their length.[30–32] In these theoretical and experimental studies, the classically nonseparable states are Bell states constructed as a superposition of elastic waves,

each being a product of a plane wave part and a spatial eigen mode. The plane wave part describes the elastic wave along the length of the waveguides, and the spatial eigen mode characterizes the amplitude and phase difference between waveguides, i.e., across the array of waveguides. In the case of a finite number of finite length waveguides, the plane wave and spatial parts are both discrete. It is therefore possible to produce elastic Bell states, whose amplitude can be represented using the usual ket notation of quantum mechanics in the form $A|S_1\rangle|k_1\rangle + D|S_2\rangle|k_2\rangle$, where $|S_i\rangle$ are discrete spatial states and $|k_j\rangle$ are discrete plane wave states. This superposition that cannot be factored as a single product is thus nonseparable. When the constitutive materials are dissipative, A and D are complex. By tuning A and D through the amplitude, phase, and/or frequency of the external drivers, one is able to experimentally navigate a portion of that Bell state Hilbert space.[30,31] However, in these previous studies, the system did not allow varying the spatial modes and plane wave states independently. This system could not be used to explore the complete Hilbert space of product elastic states because it does not support the general superposition $A|S_1\rangle|k_1\rangle + B|S_1\rangle|k_2\rangle$

$+ C|S_2\rangle|k_1\rangle + D|S_2\rangle|k_2\rangle$. Manipulation of such a general state is highly desirable as it would allow for the creation of Bell states of the form $B|S_1\rangle|k_2\rangle + C|S_2\rangle|k_1\rangle$ by tuning the complex coefficients A and D to zero. This limitation inherent to the previously studied system can be overcome by considering an externally driven system composed of a parallel array of one-dimensional elastic waveguides coupled elastically and nonuniformly along their length. In the case of waveguides coupled periodically along their length, elastic states are now products of a spatial part and a Bloch wave part. It is the objective of the present study to show that band folding within a finite Brillouin zone due to periodic coupling between waveguides offers the possibility of selecting spatial and Bloch wave states independently. Using periodically coupled one-dimensional waveguides, one can therefore navigate a more sizeable portion of the Hilbert space of nonseparable spatial mode/Bloch wave product states. Navigation of the Hilbert space of product states is achieved by stimulating externally each waveguide in the array with a driver. The product states can be tuned by varying the relative amplitude and phase of each driver as well as the frequency of the drivers.

Sections II–V introduce the theory of externally driven arrays of one-dimensional waveguides coupled periodically along their length. We present the mathematical formulation behind achieving nonseparable superpositions of states, which are the product of plane waves and spatial modes. We also show how these states can be manipulated by varying the drivers' characteristics. We demonstrate the possibility of achieving transformations between different nonseparable superpositions of product states reminiscent of nontrivial quantum gates. In Sec. VI, we introduce a mass–spring model of a parallel array of discrete waveguides coupled elastically and periodically along their length. This model is used to validate and illustrate the theory. We calculate the band structure of this model. Periodicity-induced band folding and finite length of the waveguides lead to modes that can be excited externally to realize superpositions of states that are the product of plane waves and spatial modes that span the complete available Hilbert space of product states. A section of that Hilbert space is explored by tuning the frequency and the relative amplitudes of the external drivers stimulating the individual waveguides. We show that transformation from one type of nonseparable superposition to another one in that space can be interpreted as the complex conjugation operator in the space of the complex amplitudes of individual waveguides.

II. ARRAY OF PARALLEL WAVEGUIDES COUPLED PERIODICALLY ALONG THEIR LENGTH

We consider three one-dimensional elastic waveguides coupled elastically along their length (see Fig. 1). In the long wavelength limit,
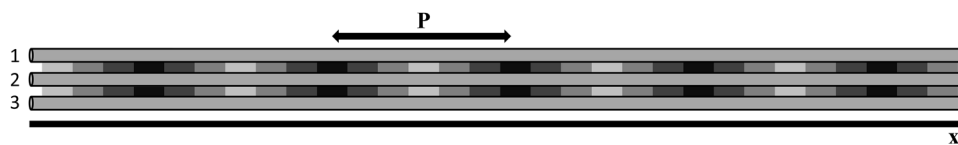
the wave equation takes the form

$$\left[\left(\frac{\partial^2}{\partial t^2} - \beta^2 \frac{\partial^2}{\partial x^2}\right)I_{3\times3} + M_{3\times3}\right]U = 0. \tag{1}$$

The parameter β is proportional to the speed of sound in the waveguides. x represents the position along the waveguides. $I_{3\times3}$ is the identity matrix. $M_{3\times3}$ is the matrix describing the elastic coupling between the three waveguides. The 3×1 vector $U = (U_1, U_2, U_3)$ represents the displacement in waveguides 1, 2, and 3, respectively.

We now assume that the coupling is periodic along the direction x. For instance, in the case of a planar array of three waveguides, the coupling matrix takes the form

$$M_{3\times3} = \alpha(x)N_{3\times3}, \tag{2}$$

where $N_{3\times3} = \begin{pmatrix} 1 & -1 & 0 \\ -1 & 2 & -1 \\ 0 & -1 & 1 \end{pmatrix}$ and $\alpha(x)$ is a periodic function with the period P. The parameter α is proportional to the stiffness of the coupling. We write the function $\alpha(x)$ as a Fourier series

$$\alpha(x) = \sum_G \alpha_G e^{iGx}, \tag{3}$$

with the reciprocal lattice number $G = m\frac{2\pi}{P}$, where m is an integer.

We seek solutions in the form of Bloch waves, namely,

$$U(x,t) = \sum_k \sum_g U(k+g)e^{i(k+g)x}e^{i\omega t}, \tag{4}$$

where g is also a reciprocal lattice number. Inserting Eqs. (2)–(4) into (1) yields

$$\sum_k \sum_g \Big\{ I_{3\times3}(-\omega^2 + \beta^2(k+g)^2)U(k+g)e^{i(k+g)x}$$
$$+ \sum_G N_{3\times3}\alpha_G U(k+g)e^{i(G+k+g)x} \Big\} = 0. \tag{5}$$

We multiply Eq. (5) by $e^{-i(k'+g')x}$ and integrate over one period $\int_0^P dx$ to obtain

$$I_{3\times3}(-\omega^2 + \beta^2(k'+g')^2)U(k'+g') + \sum_G N_{3\times3}\alpha_G U(k'+g'-G) = 0. \tag{6}$$

In obtaining Eq. (6), we have used the relation $\int dx e^{i(a-b)x} = \delta_{a,b}$, where $\delta_{a,b}$ is the usual delta function.

We now define λ_n and E_n with $n = 1, 2, 3$ as the eigenvalues and eigenvectors of the matrix $N_{3\times3}$. That is, we can write $N_{3\times3}E_n = \lambda_n I_{3\times3}E_n$. These eigenvectors are equivalent to spatial states across the parallel array of waveguides. Since E_n form a complete orthonormal basis, we can write the displacement vector as

FIG. 1. Schematic representation of three one-dimensional elastic waveguides coupled periodically along their length with a period P (stiffness of the coupling is represented schematically by different shades of gray).

$$U(k) = \sum_n u_n(k) E_n n. \tag{7}$$

Using Eq. (7), Eq. (6) becomes (here, we have dropped the prime for convenience)

$$\sum_n \Big\{ I_{3\times3} E_n \big(-\omega^2 + \beta^2(k+g)^2\big) u_n(k+g)$$
$$+ \sum_G \lambda_n I_{3\times3} E_n \alpha_G u_n(k+g-G) \Big\} = 0. \tag{8}$$

By factoring $I_{3\times3} E_n$, Eq. (8) reduces to

$$\big(-\omega^2 + \beta^2(k+g)^2\big) u_n(k+g) + \lambda_n \sum_G \alpha_G u_n(k+g-G) = 0. \tag{9}$$

This represents an infinite set of coupled equations. These equations can be solved by truncating the summation over G to a finite number of terms. For the sake of simplicity, we will examine the case when G is limited to $G = 0$ and $-\frac{2\pi}{P}$. This corresponds to periodic coupling realized as the sum of a uniform coupling parameter and one single sinusoidal function. This approximation allows for mathematical tractability while still capturing the effect of band folding due to the periodicity.

If $g = 0$, Eq. (9) simplifies to

$$\big(-\omega^2 + \beta^2 k^2\big) u_n(k) + \lambda_n \Big(\alpha_0 u_n(k) + \alpha_{-2\pi/P} u_n\Big(k + \frac{2\pi}{P}\Big) \Big) = 0. \tag{10a}$$

When $g = -\frac{2\pi}{P}$, Eq. (9) becomes

$$\Big(-\omega^2 + \beta^2 \Big(k + \frac{2\pi}{P}\Big)^2\Big) u_n\Big(k + \frac{2\pi}{P}\Big)$$
$$+ \lambda_n \Big(\alpha_0 u_n\Big(k + \frac{2\pi}{P}\Big) + \alpha_{2\pi/P} u_n(k) \Big) = 0. \tag{10b}$$

For $\alpha_{(-2\pi/P)} = \alpha^*_{2\pi/P}$, Eqs. (10a) and (10b) form the system of equations

$$\begin{pmatrix} -\omega^2 + \beta^2 k^2 + \lambda_n \alpha_0 & \lambda_n \alpha^*_{2\pi/P} \\ \lambda_n \alpha_{2\pi/P} & -\omega^2 + \beta^2 \big(k + \frac{2\pi}{P}\big)^2 + \lambda_n \alpha_0 \end{pmatrix} \begin{pmatrix} u_n(k) \\ u_n\big(k + \frac{2\pi}{P}\big) \end{pmatrix} = 0. \tag{11}$$

The dispersion relation is obtained by setting the determinant of the matrix in Eq. (11) equal to zero,

$$\big(-\omega^2 + \beta^2 k^2 + \lambda_n \alpha_0\big)\Big(-\omega^2 + \beta^2 \Big(k + \frac{2\pi}{P}\Big)^2 + \lambda_n \alpha_0\Big) - \lambda_n^2 \big|\alpha_{2\pi/P}\big|^2 = 0. \tag{12}$$

Equation (12) is rewritten as

$$\big(k^2 + \gamma_n\big)\Big(\Big(k + \frac{2\pi}{P}\Big)^2 + \gamma_n\Big) - \eta_n^2 = 0 \tag{13}$$

by defining $\gamma_n = \frac{\lambda_n \alpha_0 - \omega^2}{\beta^2}$ and $\eta_n^2 = \frac{\lambda_n^2 \big|\alpha_{2\pi/P}\big|^2}{\beta^2}$.

The four solutions of Eq. (13) are given in the compact form as

$$k_n(\omega) = -\frac{\pi}{P} \pm \sqrt{\Big(\frac{\pi}{P}\Big)^2 - \gamma_n \pm \sqrt{\eta_n^2 - \Big(\frac{2\pi}{P}\Big)^2 \gamma_n}}. \tag{14}$$

For a given ω, and n, two wave numbers correspond to the $G = 0$ dispersion curves. The other two wave numbers are associated with the dispersion curves translated by the reciprocal number $G = -\frac{2\pi}{P}$ (see Fig. 2), i.e., dispersion curves translated into the second Brillouin zone to the left of the first Brillouin zone. Equivalently, these latter
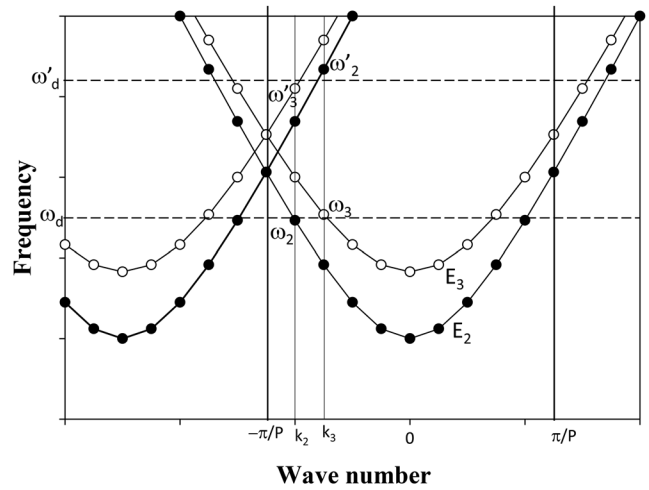

FIG. 2. Schematic representation of the dispersion curves for the two eigen modes E_2 and E_3 (closed and open circles) with $g = 0, \frac{2\pi}{P}$ and their corresponding discrete states. The first Brillouin zone is delimited by vertical lines at $-\frac{\pi}{P}$ and $\frac{\pi}{P}$. The driving frequencies ω_D and ω'_D are represented as a horizontal dashed line. The wave numbers k_2 and k_3 and corresponding characteristic frequencies $\omega_2, \omega_3, \omega'_2$, and ω'_3 are labeled. The gaps that may have formed at $k = -\frac{\pi}{P}$ are not represented for the sake of simplifying the illustration. The length of the finite waveguides is $L = 5P$.

wave numbers correspond to dispersion branches, which fold within the first Brillouin zone. If more G vectors were kept in the calculation, the band structure would include dispersion curves translated not only in the second Brillouin zone but also in third, fourth, and higher order Brillouin zones. The extension of this translated dispersion relation would be equivalent to multiple folding of the bands in the first Brillouin zone. However, a single band folding is sufficient here to illustrate the condition for observing a nonseparable superposition of states spanning the complete Hilbert space of product states.

It is worth analyzing Eq. (14) in a few simple cases. In the absence of periodicity in the coupling between the waveguides, $\alpha_{2\pi/P} = 0$ and $\eta_n^2 = 0$. Equation (12) reduces to the two dispersion relations $\omega^2 = \beta^2 k^2 + \lambda_n \alpha_0$ and $\omega^2 = \beta^2 \big(k + \frac{2\pi}{P}\big)^2 + \lambda_n \alpha_0$. These are the dispersion relations for waveguides coupled uniformly along their length in a supercell of length P. Note that in that case at $k = 0$ and $k = -\frac{2\pi}{P}$, the lowest positive and real frequencies are given by $\omega^2 = \lambda_n \alpha_0$.

For the system with periodic coupling, if we insert the condition $\omega^2 = \lambda_n \alpha_0$ (i.e., $\gamma_n = 0$) in Eq. (14), we find four nonzero solutions for the wave number $k_n(\omega) = -\frac{\pi}{P} \pm \sqrt{\big(\frac{\pi}{P}\big)^2 \pm \eta_n}$. This indicates that in the vicinity of the wave number origin, the bands of the periodically coupled systems have been lowered compared to those of the uniformly coupled system. Finally, at the edge of the Brillouin zone, $k = -\frac{\pi}{P}$, Eq. (14) gives the following condition: $\big(\big(\frac{\pi}{P}\big)^2 + \gamma_n\big)^2 = \eta_n^2$ or $\omega^2 = \lambda_n\big(\alpha_0 \mp \beta\alpha_{2\pi/P}\big) + \beta^2\big(\frac{\pi}{P}\big)^2$. At the edge of the Brillouin zone, the degeneracy of the folded bands is lifted by opening a gap. For instance, the positive frequency at $k = -\frac{\pi}{P}$ is two valued.

III. DRIVEN ARRAY OF ELASTIC WAVEGUIDES COUPLED PERIODICALLY ALONG THEIR LENGTH

Let us now drive the system externally at some position $x = 0$. Equation (1) is replaced by

$$\left[\left(\frac{\partial^2}{\partial t^2} - \beta^2 \frac{\partial^2}{\partial x^2}\right)I_{3\times3} + M_{3\times3}\right]U = F\delta_{x=0}e^{i\omega_D t}, \quad (15)$$

where ω_D is the frequency of the driver. The 3×1 vector, F, is expressed in the E_n basis: $F = \sum_n F_n E_n$. The F_n's are therefore defined as the dot product $F \cdot E_n$ between the two 3×1 vectors.

Again, we seek solutions in the form of Bloch waves with the driver's frequency,

$$U_D(x,t) = \sum_k \sum_g \sum_n u_{D,n}(k+g)E_n e^{i(k+g)x}e^{i\omega_D t}. \quad (16)$$

The index D of $u_{D,n}$ indicates that this is the amplitude of the driven system.

Following the algebraic steps of Sec. II, we obtain the set of equations

$$\left(-\omega_D^2 + \beta^2(k+g)^2\right)u_{D,n}(k+g) + \lambda_n \sum_G \alpha_G u_{D,n}(k+g-G) = F_n. \quad (17)$$

In obtaining the right-hand side of Eq. (17), we have used $F\int dx e^{-i(k'+g')x}\delta_{x=0} = F$. Similarly to Sec. II, Eq. (17) represents an infinite set of coupled equations.

Again, limiting the reciprocal lattice numbers to $G = 0$ and $-\frac{2\pi}{P}$, and $g = 0$ and $\frac{2\pi}{P}$, we obtain the set of two linear equations

$$\begin{pmatrix} -\omega_D^2 + \beta^2 k^2 + \lambda_n\alpha_0 & \lambda_n\alpha^*_{2\pi/P} \\ \lambda_n\alpha_{2\pi/P} & -\omega_D^2 + \beta^2\left(k+\frac{2\pi}{P}\right)^2 + \lambda_n\alpha_0 \end{pmatrix}$$
$$\times \begin{pmatrix} u_{D,n}(k) \\ u_{D,n}\left(k+\frac{2\pi}{P}\right) \end{pmatrix} = \begin{pmatrix} F_n \\ F_n \end{pmatrix}. \quad (18)$$

The driven resonant amplitudes are therefore given by

$$\begin{pmatrix} u_{D,n}(k) \\ u_{D,n}\left(k+\frac{2\pi}{P}\right) \end{pmatrix} = \frac{1}{\Delta_n}\begin{pmatrix} -\omega_D^2 + \beta^2\left(k+\frac{2\pi}{P}\right)^2 + \lambda_n\alpha_0 & -\lambda_n\alpha^*_{2\pi/P} \\ -\lambda_n\alpha_{2\pi/P} & -\omega_D^2 + \beta^2 k^2 + \lambda_n\alpha_0 \end{pmatrix}$$
$$\times F_n\begin{pmatrix} 1 \\ 1 \end{pmatrix}, \quad (19)$$

where

$$\Delta_n = \left(-\omega_D^2 + \beta^2 k^2 + \lambda_n\alpha_0\right)\left(-\omega_D^2 + \beta^2\left(k+\frac{2\pi}{P}\right)^2 + \lambda_n\alpha_0\right) - \lambda_n^2\left|\alpha_{2\pi/P}\right|^2.$$

If we employ Eq. (12), we can express the denominator, Δ_n, as

$$\Delta_n = \left(-\omega_D^2 + \beta^2 k^2 + \lambda_n\alpha_0\right)\left(-\omega_D^2 + \beta^2\left(k+\frac{2\pi}{P}\right)^2 + \lambda_n\alpha_0\right)$$
$$- \left(-\omega_n^2 + \beta^2 k^2 + \lambda_n\alpha_0\right)\left(-\omega_{n,P}^2 + \beta^2\left(k+\frac{2\pi}{P}\right)^2 + \lambda_n\alpha_0\right), \quad (20)$$

where ω_n and $\omega_{n,P}$ are the characteristic frequencies corresponding to the nth eigen mode of the coupling matrix with the wave numbers k and $k+\frac{2\pi}{P}$ [see Eq. (14)]. If the system exhibits some damping, taking the form $\eta\frac{\partial}{\partial t}$, where η is a damping coefficient, in Eq. (15),

one needs to replace ω_D^2 by $\omega_D^2 - i\eta\omega_D$. Importantly, in that case, the amplitudes $\begin{pmatrix} u_{D,n}(k) \\ u_{D,n}\left(k+\frac{2\pi}{P}\right) \end{pmatrix}$ are complex quantities. Complex amplitudes are important to establish the analogy between nonseparable elastic states and locally "entangled" quantum states described in Sec. IV.

IV. NONSEPARABLE ELASTIC STATES SUPPORTED BY THE PERIODICALLY COUPLED WAVEGUIDES

Here, we demonstrate that the displacement field of the driven system can be written as nonseparable superposition of states. Solving Eq. (17) by truncating the sum over the reciprocal lattice number beyond what was done in Sec. III would result in complex driven amplitudes $u_{D,n}(k+g)$. These complex amplitudes are proportional to F_n, so we rewrite them as

$$u_{D,n}(k+g) = F_n\tilde{u}_{D,n}(k+g). \quad (21)$$

In the case of the three waveguides arranged in a planar array, the coupling matrix $N_{3\times3}$ admits three eigen vectors and three eigen values. One of the eigen vectors for which $\lambda_1 = 0$, namely, $E_1 = \frac{1}{\sqrt{3}}(1,1,1)$, does not involve transfer of energy between the waveguides via the coupling. This trivial case is equivalent to three independent waveguides. The other two eigen modes of the coupling matrix with eigen values $\lambda_2 = 1$ and $\lambda_3 = 3$ are

$$E_2 = \frac{1}{\sqrt{2}}\begin{pmatrix} 1 \\ 0 \\ -1 \end{pmatrix}, \quad E_3 = \frac{1}{\sqrt{6}}\begin{pmatrix} 1 \\ -2 \\ 1 \end{pmatrix}. \quad (22)$$

We now suppose that we are driving the system with $F_1 = 0$ (to eliminate the E_1 mode) and $F_2 \neq F_3 \neq 0$. The displacement field of Eq. (16) becomes

$$U_D(x,t) = \sum_k \sum_g \left[F_2\tilde{u}_{D,2}(k+g)E_2 + F_3\tilde{u}_{D,3}(k+g)E_3\right]e^{i(k+g)x}e^{i\omega_D t}. \quad (23)$$

We note that in Eq. (23), we use a discrete summation over the wave number k. This condition can be realized with finite length waveguides obeying periodic boundary conditions. This system supports a discrete set of standing waves. Furthermore, let us suppose that ω_D is close to two characteristic frequencies ω_2 and ω_3 corresponding to the second and third eigen modes of the coupling matrix with the wave numbers k_2 and k_3 inside the first Brillouin zone and $k_2 + g$ and $k_3 + g$ inside the other Brillouin zones, respectively (see Fig. 2). The amplitudes $\tilde{u}_{D,2}(k_2+g)$ and $\tilde{u}_{D,3}(k_3+g)$ are expected to dominate, and the sum over k in Eq. (23) can be approximated as

$$U_D(x,t) = \sum_g \Big[F_2\tilde{u}_{D,2}(k_2+g)E_2 e^{i(k_2+g)x}$$
$$+ F_3\tilde{u}_{D,3}(k_3+g)E_3 e^{i(k_3+g)x}\Big]e^{i\omega_D t}. \quad (24)$$

The choice of the driving frequency ω_D determines how many waves with different k will be composing the superposition of states given by Eq. (23).

For each g, we define the orthonormal basis $\phi_1 = E_2 e^{i(k_2+g)x}$, $\phi_2 = E_2 e^{i(k_3+g)x}$, $\phi_3 = E_3 e^{i(k_2+g)x}$, and $\phi_4 = E_3 e^{i(k_3+g)x}$. Using the bracket notation, we can define $|\phi_1\rangle = |E_2\rangle|k_2\rangle$, $|\phi_2\rangle = |E_2\rangle|k_3\rangle$, $|\phi_3\rangle = |E_3\rangle|k_2\rangle$, and $|\phi_4\rangle = |E_3\rangle|k_3\rangle$. The two vectors $|E_2\rangle$

and $|E_3\rangle$ form an orthonormal basis for a two-dimensional Hilbert space H_E. $|k_2\rangle = e^{i(k_2+g)x}$ and $|k_3\rangle = e^{i(k_3+g)x}$ form another orthonormal basis for a two-dimensional Hilbert space H_k. $|\phi_1\rangle$, $|\phi_2\rangle$, $|\phi_3\rangle$, and $|\phi_4\rangle$ form the basis of a four-dimensional Hilbert product space $H_{E,k} = H_E \otimes H_k$. In that basis, U_D takes the form

$$U_D(x,t) = \sum_g [F_2 \tilde{u}_{D,2}(k_2+g)\phi_1 + F_3 \tilde{u}_{D,3}(k_3+g)\phi_4]e^{i\omega_D t}. \quad (25)$$

The displacement field is a linear combination of nonseparable states. Indeed, we cannot write $F_2 \tilde{u}_{D,2}(k_2+g)\phi_1 + F_3 \tilde{u}_{D,3}(k_3+g)\phi_4$ as a product of the form $(aE_2 + bE_3)\left(ce^{i(k_2+g)x} + de^{i(k_3+g)x}\right)$, where the first parenthesis is a linear combination of E_n's and the second parenthesis is a linear combination of Bloch wave components.

If we change the driving frequency from ω_d to ω'_d such that now the largest amplitude $\tilde{u}_{D',2}$ occurs at the characteristic frequencies ω'_2 with the wave number k_3 or $k_3 + g$ and the largest amplitude $\tilde{u}_{D',3}$ occurs at ω'_3 and k_2 or $k_2 + g$ (Fig. 2), then the displacement field takes the new form

$$U_{D'}(x,t) = \sum_g \Big[F_2 \tilde{u}_{D',2}(k_3+g)E_2 e^{i(k_3+g)x}$$
$$+ F_3 \tilde{u}_{D',3}(k_2+g)E_3 e^{i(k_2+g)x} \Big] e^{i\omega'_D t}. \quad (26)$$

Equation (26) can be expressed in terms of the product basis,

$$U_{D'}(x,t) = \sum_g [F_2 \tilde{u}_{D',2}(k_3+g)\phi_2 + F_3 \tilde{u}_{D',3}(k_2+g)\phi_3]e^{i\omega'_D t}. \quad (27)$$

We can simplify these expressions further by considering that the measurements of the displacement fields given by Eqs. (25) and (26) are performed at a distance $x = QP$, where Q is an integer, from the driver. In that case, $\phi_{1,P} = E_2 e^{ik_2 QP}$, $\phi_{2,P} = E_2 e^{ik_3 QP}$, $\phi_{3,P} = E_3 e^{ik_2 QP}$, and $\phi_{4,P} = E_3 e^{ik_3 QP}$. The product basis becomes independent of the reciprocal lattice number, g, since $e^{igQP} = 1$. The displacement fields are then reduced to

$$U_D(QP,t) = \left\{ \Big[\sum_g F_2 \tilde{u}_{D,2}(k_2+g) \Big]\phi_{1,P} \right.$$
$$\left. + \Big[\sum_g F_3 \tilde{u}_{D,3}(k_3+g) \Big]\phi_{4,P} \right\}e^{i\omega_D t}, \quad (28a)$$

$$U_{D'}(QP,t) = \left\{ \Big[\sum_g F_2 \tilde{u}_{D',2}(k_3+g) \Big]\phi_{2,P} \right.$$
$$\left. + \Big[\sum_g F_3 \tilde{u}_{D',3}(k_2+g) \Big]\phi_{3,P} \right\}e^{i\omega'_D t}. \quad (28b)$$

The amplitudes of $U_D(QP,t)$ and $U_{D'}(QP,t)$ take the form of nonseparable linear combinations of product states. Equations (28a) and (28b) are isomorphic to Bell states. By controlling the driving frequency, one is able to navigate the Hilbert space $H_{E,k}$ by transforming a state of the form $A|E_2\rangle|k_2\rangle + D|E_3\rangle|k_3\rangle$ into a state of the form $B|E_2\rangle|k_3\rangle + C|E_3\rangle|k_2\rangle$, where A, B, C, D are complex amplitudes. Without the periodicity of the coupling, that is, without the folding of the bands within the first Brillouin zone (or, equivalently, the translation of bands within the second Brillouin zone), the state $B|E_2\rangle|k_3\rangle + C|E_3\rangle|k_2\rangle$ would not be accessible to observation.

Navigation of the Hilbert space enables transformation of states analogous to quantum gates. For instance, we can also define the basis $\{\phi_{1,P}, \phi_{2,P}, \phi_{3,P}, \phi_{4,P}\}$ in terms of the 4×1 vectors

$$\begin{pmatrix}1\\0\\0\\0\end{pmatrix}, \begin{pmatrix}0\\1\\0\\0\end{pmatrix}, \begin{pmatrix}0\\0\\1\\0\end{pmatrix}, \begin{pmatrix}0\\0\\0\\1\end{pmatrix}.$$ In that representation, the two displacement fields become

$$U_D(QP,t) = \begin{pmatrix}\sum_g F_2 \tilde{u}_{D,2}(k_2+g)\\0\\0\\\sum_g F_3 \tilde{u}_{D,3}(k_3+g)\end{pmatrix} e^{i\omega_D t} = \begin{pmatrix}A_{2,2}\\0\\0\\A_{3,3}\end{pmatrix} e^{i\omega_D t}, \quad (29a)$$

$$U_{D'}(QP,t) = \begin{pmatrix}0\\\sum_g F_2 \tilde{u}_{D',2}(k_3+g)\\\sum_g F_3 \tilde{u}_{D',3}(k_2+g)\\0\end{pmatrix} e^{i\omega'_D t} = \begin{pmatrix}0\\A_{2,3}\\A_{3,2}\\0\end{pmatrix} e^{i\omega'_D t}. \quad (29b)$$

Changing the driving frequency from ω_D to ω'_D is therefore equivalent to applying the following transformation matrix to the amplitude vectors:

$$\begin{pmatrix}0\\A_{2,3}\\A_{3,2}\\0\end{pmatrix} = \begin{pmatrix}0 & A_{2,3}/A_{2,2} & 0 & 0\\A_{2,3}/A_{2,2} & 0 & 0 & 0\\0 & 0 & 0 & A_{3,2}/A_{3,3}\\0 & 0 & A_{3,2}/A_{3,3} & 0\end{pmatrix}\begin{pmatrix}A_{2,2}\\0\\0\\A_{3,3}\end{pmatrix}. \quad (30)$$

The most significant aspect of this transformation matrix is that it contains non-zero off-diagonal terms of the two blocks. The physical effects of this transformation are directly measurable in terms of amplitudes and relative phases of the waveguide displacement at the location $x = QP$.

For instance, one measures the three components $(U_{1,D}(QP,t), U_{2,D}(QP,t), U_{3,D}(QP,t))$ and expresses them as $(G_1, G_2 e^{i\phi_{12}}, G_3 e^{i\phi_{13}})$, where ϕ_{12} and ϕ_{13} are the phases of the displacement of waveguides 2 and 3 relative to waveguide 1. If the amplitude of the first waveguide is normalized to 1, the four quantities G_2, G_3, ϕ_{12}, and ϕ_{13} completely characterize the nonseparable state given by Eq. (29a). Similarly, we can characterize the nonseparable state $U_{D'}(QP,t)$ with two other relative amplitudes and two relative phases G'_2, G'_3, ϕ'_{12}, and ϕ'_{13}.

We also note that the complex quantities $A_{2,2}$ and $A_{3,3}$ can be tuned via the control of the driver amplitudes F_2 and F_3 and their relative phase. The same is true for the quantities $A_{2,3}$ and $A_{3,2}$. Indeed, rewriting $F_2 = |F_2|$ and $F_3 = |F_3|e^{i\theta}$, where θ is the phase difference between F_2 and F_3, we can add θ to the phase difference between $\sum_g \tilde{u}_{D,2}(k_2+g)$ and $\sum_g \tilde{u}_{D,3}(k_3+g)$ when driving at ω_D. A similar phase difference can be added between $\sum_g \tilde{u}_{D',2}(k_3+g)$ and $\sum_g \tilde{u}_{D',3}(k_2+g)$ when driving at ω'_D. Control of the frequency of the drivers and their relative phase provides significant flexibility to manipulate the coefficients of the transformation matrix given by Eq. (30). The significance of the transformation matrix in Eq. (30) is its nonzero off-diagonal terms. With appropriate tuning of the complex amplitudes via the external drivers or of the geometry of an array of waveguides or physical characteristics of the constitutive materials, one may be able to achieve elastic generalized analogs of nontrivial quantum gates such as the Pauli X gate.

V. NAVIGATING THE COMPLETE HILBERT SPACE, $H_{E,k}$

To navigate the space, $H_{E,k}$, we need to excite four amplitudes simultaneously with a single driving frequency, to obtain a displacement field of the form

$$U_D(QP, t) = (B_{2,2}\phi_{1,P} + B_{2,3}\phi_{2,P} + B_{3,2}\phi_{3,P} + B_{3,3}\phi_{4,P})e^{i\omega_d t}. \quad (31)$$

One can excite such a state in the vicinity of a crossing point between the bands corresponding to the coupling modes, E_2 and E_3. The crossing occurs between the E_2 band with $g = \frac{2\pi}{P}$ and the E_3 band with $g = 0$. Using Eq. (14), such a crossing occurs at $k_2(\omega) = k_3(\omega)$. The continuous bands in Fig. 2 exhibit such a crossing point. In the case of finite length waveguides with periodic boundary conditions, and driving the system with a frequency near the crossing point frequency, Eq. (23) can be simplified into the following form:

$$U_D(x, t) = \sum_g \Big[F_2 \tilde{u}_{D,2}(k_2 + g) E_2 e^{i(k_2 + g)x}$$
$$+ F_2 \tilde{u}_{D,2}\left(-\frac{\pi}{P} + g\right) E_2 e^{i(-\frac{\pi}{P} + g)x}$$
$$+ F_3 \tilde{u}_{D,3}\left(-\frac{\pi}{P} + g\right) E_3 e^{i(-\frac{\pi}{P} + g)x}$$
$$+ F_3 \tilde{u}_{D,3}(k_2 + g) E_3 e^{i(k_2 + g)x} \Big] e^{i\omega_D t}. \quad (32)$$

To obtain Eq. (23), we are assuming that only four classes of points in the vicinity of the crossing point frequency contribute significantly to the amplitude of the displacement field. The resonant frequency associated with these points is the closest to the driving frequency. Again, performing measurements at $x = QP$, where Q is an integer, from the driver, using $e^{igQP} = 1$, and defining the basis $\phi_{1,P} = E_2 e^{ik_2 QP}$, $\phi_{2,P} = E_2 e^{i(-\frac{\pi}{P})QP}$, $\phi_{3,P} = E_3 e^{i(-\frac{\pi}{P})QP}$, and $\phi_{4,P} = E_3 e^{ik_2 QP}$, Eq. (32) becomes

$$U_D(QP, t) = \Big\{ \Big[\sum_g F_2 \tilde{u}_{D,2}(k_2 + g) \Big] \phi_{1,P} + \Big[\sum_g F_2 \tilde{u}_{D,2}\left(-\frac{\pi}{P} + g\right) \Big] \phi_{2,P}$$
$$+ \Big[\sum_g F_3 \tilde{u}_{D,3}\left(-\frac{\pi}{P} + g\right) \Big] \phi_{3,P}$$
$$+ \Big[\sum_g F_3 \tilde{u}_{D,3}(k_2 + g) \Big] \phi_{4,P} \Big\} e^{i\omega_D t}. \quad (33)$$

This equation can be rewritten in the desirable form of Eq. (31) by defining $B_{2,2} = \Big[\sum_g F_2 \tilde{u}_{D,2}(k_2 + g) \Big]$, $B_{2,3} = \Big[\sum_g F_2 \tilde{u}_{D,2}\left(-\frac{\pi}{P} + g\right) \Big]$, $B_{3,2} = \Big[\sum_g F_3 \tilde{u}_{D,3}\left(-\frac{\pi}{P} + g\right) \Big]$, and $B_{3,3} = \Big[\sum_g F_3 \tilde{u}_{D,3}(k_2 + g) \Big]$. In the bracket notation, this state takes the general form $A|E_2\rangle|k_2\rangle + B|E_2\rangle|k_3\rangle + C|E_3\rangle|k_2\rangle + D|E_3\rangle|k_3\rangle$. Such a state would not be accessible without the folding of the bands resulting from the periodicity of the coupling.

The product Hilbert space can be explored by changing the frequency to values above or below the frequency of the crossing point. This effectively changes the complex coefficients A, B, C, D. The magnitude and relative phase of F_2 and F_3 offer additional degrees of freedom to manipulate the complex amplitudes of the superposition of states.

By tuning the magnitude of the coupling stiffness as well as the length of the finite waveguides (with periodic boundary conditions), one can create more general states. For instance, in Fig. 3, we are schematically representing $g = 0$ and $\frac{2\pi}{P}$ for two E_2 and E_3 bands in the case of finite length waveguides $L = 9P$. In this particular case, we have four classes of modes a, b, c, and d flanking a crossing point
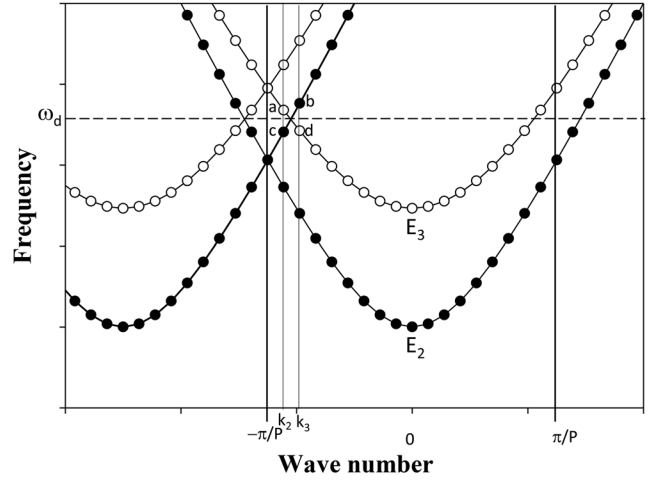

FIG. 3. Schematic representation of the dispersion curves for the two eigen modes E_2 and E_3 (closed and open circles) with $g = 0$, $\frac{2\pi}{P}$ and their corresponding discrete states. Here, the length of the finite waveguides is $L = 9P$. The first Brillouin zone is delimited by vertical lines at $-\frac{\pi}{P}$ and $\frac{\pi}{P}$. The driving frequency ω_D is represented as a horizontal dashed line. The wave numbers k_2 and k_3 correspond to the E_3 (a) and E_2 (c) modes and E_2 (b) and E_3 (d) modes, respectively. The gaps that may have formed at $k = -\frac{\pi}{P}$ are not represented for the sake of simplifying the illustration.

within the first Brillouin zone. Driving the system at the frequency ω_D shown in the figure, the measured displacement field at QP will take the form

$$U_D(QP, t) = \Big\{ \Big[\sum_g F_2 \tilde{u}_{D,2}(k_2 + g) \Big] \phi_{1,P} + \Big[\sum_g F_2 \tilde{u}_{D,2}(k_3 + g) \Big] \phi_{2,P}$$
$$+ \Big[\sum_g F_3 \tilde{u}_{D,3}(k_2 + g) \Big] \phi_{3,P}$$
$$+ \Big[\sum_g F_3 \tilde{u}_{D,3}(k_3 + g) \Big] \phi_{4,P} \Big\} e^{i\omega_D t}, \quad (34)$$

with the product basis $\phi_{1,P} = E_2 e^{ik_2 QP}$, $\phi_{2,P} = E_2 e^{ik_3 QP}$, $\phi_{3,P} = E_3 e^{ik_2 QP}$, and $\phi_{4,P} = E_3 e^{ik_3 QP}$.

By driving the system at a frequency, $\omega_D^{(a,b)}$ in the vicinity of the frequencies of the two modes a and b, the primary contributions to the resonant displacement field are limited to $U_D^{(a,b)}(QP, t) = \Big\{ \Big[\sum_g F_2 \tilde{u}_{D,2}(k_3 + g) \Big] \phi_{2,P} + \Big[\sum_g F_3 \tilde{u}_{D,3}(k_2 + g) \Big] \phi_{3,P} \Big\} e^{i\omega_d^{(a,b)} t}$. This state is not separable. If we then tune the driving frequency to a value, $\omega_D^{(c,d)}$ in the vicinity of those of the modes c and d, the primary contributions to the displacement field are reduced to $U_D^{(c,d)}(QP, t) = \Big\{ \Big[\sum_g F_2 \tilde{u}_{D,2}(k_2 + g) \Big] \phi_{1,P} + \Big[\sum_g F_3 \tilde{u}_{D,3}(k_3 + g) \Big] \phi_{4,P} \Big\} e^{i\omega_d^{(c,d)} t}$. This is also a nonseparable state. The transition from one of these nonseparable states to the other one is solely allowed by the band folding due to the periodicity of the coupling.

We note that Eq. (34) becomes separable if we can find a driving frequency such that

$$\sum_g \tilde{u}_{D,2}(k_2 + g) = \sum_g \tilde{u}_{D,3}(k_2 + g) = D_2,$$

$$\sum_g \tilde{u}_{D,2}(k_3 + g) = \sum_g \tilde{u}_{D,3}(k_3 + g) = D_3.$$

Then, Eq. (34) can be written in the product form

$$U_D(QP, t) = \left\{ (F_2 E_2 + F_3 E_3)\left(D_2 e^{ik_2 QP} + D_3 e^{ik_3 QP} \right) \right\} e^{i\omega_D t}. \quad (35)$$

The relative amplitudes and phase of the three components $(U_{1,D}(QP, t), U_{2,D}(QP, t), U_{3,D}(QP, t))$ expressed as $(G_1, G_2 e^{i\phi_{12}}, G_3 e^{i\phi_{13}})$ are simply dependent on the factor $F_2 E_2 + F_3 E_3$. The factor $(D_2 e^{ik_2 QP} + D_3 e^{ik_3 QP})$ only adds a global phase to each waveguide. The phases of the displacement of waveguides 2 and 3 relative to waveguide 1 parallel the relative phase of the external drivers. This is a signature of separability of the elastic states. Nonseparable states will exhibit relative phases between waveguides, which differ from the relative phase of the drivers. It is therefore possible with this simple measurement to differentiate nonseparable from separable superpositions of elastic states.

Finally, we also recall that in the model system composed of three coupled waveguides, there are only two non-trivial discrete eigen vectors describing the spatial states, namely, E_2 and E_3. This represents, effectively, a two-level system. Furthermore, due to the finite length of the waveguides, the plane wave states are discrete. We have chosen driving frequencies such that only two plane wave states may contribute the most to the displacement field. The system behaves like a two-level system in plane wave states. The Hilbert space of this restricted system is therefore a 2×2 dimensional space. The periodicity of the coupling between waveguides, leading to band folding, enables the complete exploration of this Hilbert space. Increasing the number of coupled waveguides will increase the number of non-trivial spatial eigen modes. For instance, in the case of four coupled waveguides, the spatial states represent a three-level system. The spatial states of N coupled waveguides would span an $N - 1$ dimensional space. By increasing the length of the waveguides, one increases the number of discrete plane wave states within a given range of frequencies. It is therefore possible to extend the space of dominant plane wave states beyond the two investigated here. For instance, one can consider a driving frequency that would excite three plane wave states with significant amplitudes. In that case, the plane wave states would span a three-dimensional space corresponding to a three-level system. Generalizing to n plane wave states corresponding to an n-level system, an elastic system of N waveguides could support superpositions of states in an $(N - 1) \times n$ Hilbert space of product states.

VI. COMPUTER MODEL AND SIMULATION

To validate the theory in Sec. V, we develop a numerical model based on coupled mass–spring waveguides that can be used to shed light on the complex behavior of nonseparable states and hence on the complex Hilbert space, $H_{E,k}$. For this, we consider a set of 1D discrete elastic waveguides composed of chains of identical masses connected to each other via harmonic springs. We further assume that the masses of each chain are constrained to move only in the horizontal direction. This limits the model to displacements with a single polarization as was the case in Sec. V. Dissipative effects in the medium are modeled by linear viscous damping elements.

For a set of three coupled mass–spring chains with a total of N_m identical masses in each chain, the discrete elastic equations of

motion are given by

$$m\ddot{u}_n - k_{nn}(u_{n+1} - 2u_n + u_{n-1}) - k_c(v_n - u_n) + \eta\dot{u}_n = 0, \quad (36a)$$

$$m\ddot{v}_n - k_{nn}(v_{n+1} - 2v_n + v_{n-1}) - k_c(u_n - v_n) - k_c(w_n - v_n) + \eta\dot{v}_n = 0, \quad (36b)$$

$$m\ddot{w}_n - k_{nn}(w_{n+1} - 2w_n + w_{n-1}) - k_c(v_n - w_n) + \eta\dot{w}_n = 0, \quad (36c)$$

where u_n, v_n, and w_n are the displacements of the nth mass of waveguides 1, 2, and 3, respectively. These quantities form the spatially discrete components of the 3×1 vector U used in Secs. II–V for a continuous system. m is the mass, and the viscous damping coefficient η models the dissipation. The term k_{nn} describes the coupling constant of the nearest-neighbor interaction along a waveguide, and k_c describes the stiffness of the springs that couple the masses between the waveguides organized in a planar array. The spring constant k_c has a sinusoidal modulation so that

$$k_c = k_{c,0}\left(1 + \Delta k_c \sin\left(\frac{2\pi}{P} x_n\right)\right), \quad (37)$$

where $k_{c,0}$ is the unmodulated spring constant and $\Delta k_c k_{c,0}$ is the modulation amplitude. Here, we take k_c to be the same for all coupled chains. The superposition of a constant coupling stiffness and a simple sinusoidal variation parallels our choice of reciprocal numbers limited to the two values $G = 0$ and $-\frac{2\pi}{P}$ in Secs. II–V.

We use Born–von Karman periodic boundary conditions for which $e^{ikN_c P} = 1$; N_c is the total number of unit cells along the waveguides. As mentioned above, in the first Brillouin zone, kP is limited to the interval $-\pi$ to π with a spacing of $2\pi/N_c$. The set of Eqs. (36a)–(36c) is the discrete equivalent of Eq. (1). A vectorized fourth order Runge–Kutta time integration scheme is used to numerically calculate the dynamics of the system. To computationally generate the band structure, the spectral analysis of amplitudes and phases method[24] is employed, which we have recently developed and entails the use of molecular dynamics simulation. The band structure in the absence of damping is reported in Fig. 4. The specific values of the model physical constants are presented in the figure caption. From Fig. 4, it is clear that the E_1 mode does not involve transfer of energy between the waveguides via the coupling and hence does not fold in the Brillouin zone. On the other hand, near the edges of the first Brillouin zone, the bands corresponding to the E_2 and E_3 spatial eigen modes fold and hence intersect. Because of the finite length of the waveguides, four discrete modes (two closed and two open circle modes) near these intersections form two pairs of modes with the same wave numbers. This configuration is isomorphic to that schematically presented in Fig. 3.

Each mode represented by a single closed or open circle in the band structure of Fig. 4 corresponds to a separable state in the Hilbert space $H_{E,k}$, i.e., states expressible as products of eigen modes spatially varying across the array of waveguides and Bloch wave degrees of freedom along the waveguides. From Fig. 4, we identify different isofrequency values that correspond to nearly overlapping E_2 and E_3 modes. For instance, the inset of Fig. 4 shows that driving the model at a frequency of 0.622 or 0.6 will lead to non-separable superpositions of states with characteristics similar to those of the theoretical superpositions $U_D^{(a,b)}$ or
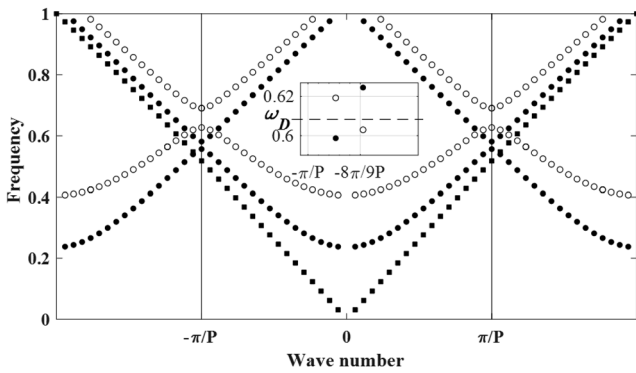
FIG. 4. Elastic wave band structure of three-discrete mass–spring waveguides coupled along their length via a periodic sinusoidal modulation of coupling stiffness. The closed circles correspond to resonant modes associated with the E_2 spatial eigen mode, and the open circles correspond to resonant modes associated with the E_3 spatial eigen mode. The E_1 eigen mode corresponds to closed squares in the plot. The dashed line in the inset identifies a frequency (ω_D) at which the E_2 and E_3 resonances nearly overlap with two pairs of identical wave number: $\omega_a = 0.6193$, $\omega_b = 0.6246$, $\omega_c = 0.5987$, $\omega_d = 0.6030$. The first Brillouin zone is represented by vertical lines at $-\frac{\pi}{P}$ and $\frac{\pi}{P}$. Dimensionless system parameters are $m = 1, N_c = 204, P = 6, k_{c,0} = 0.056, \Delta k_c = 0.50, \eta = 0$.

$U_D^{(c,d)}$ with either two or four frequency values: $\omega_a = 0.6193$, $\omega_b = 0.6246, \omega_c = 0.5987, \omega_d = 0.6030$, and two wave number values: $k_{a,c} = -16(2\pi/N_c)$, $k_{b,d} = -15(2\pi/N_c)$. We can therefore use these frequencies to numerically realize nonseparable superposition of states in $H_{E,k}$. Driving the model at a frequency between 0.622 and 0.6 will lead to linear superpositions of states $U_D^{(a,b)}$ and $U_D^{(c,d)}$. To excite such separable or nonseparable superpositions of states numerically, the coupled elastic system is driven with the external force $\vec{F}e^{i\omega_d t}$; $\vec{F} = (1 - \mu)E_2 + \mu E_3$. Moreover, by tuning the parameter μ, the contribution of the two eigen modes (E_2, E_3) is numerically manipulated. Finally, to drive the system, the prescribed base periodic excitation $F^u(t) = F_0^u \sin(\omega_d t + \phi_0^u), F^v(t) = F_0^v \sin(\omega_d t + \phi_0^v)$, and $F^w(t) = F_0^w \sin(\omega_d t + \phi_0^w)$ is applied to the first mass of each chain, where (F_0^u, F_0^v, F_0^w) and $(\phi_0^u, \phi_0^v, \phi_0^w)$ are the amplitudes and phases of the applied force to the chain (1, 2, 3).

Figure 5 shows the variations of the maximum amplitudes of the last mass of each waveguide C_i; $C_1 = \max(u_{N_m}(t)), C_2 = \max(v_{N_m}(t)), C_3 = \max(w_{N_m}(t))$ and the phase difference (ϕ_{ij}) between the transmissions for each pair of waveguides as a function of μ, where $\phi_{12} = \frac{180}{\pi}\cos^{-1}\left(\frac{u_{N_m}(t) \cdot v_{N_m}(t)}{|u_{N_m}(t)||v_{N_m}(t)|}\right)$, $\phi_{23} = \frac{180}{\pi}\cos^{-1}\left(\frac{v_{N_m}(t) \cdot w_{N_m}(t)}{|v_{N_m}(t)||w_{N_m}(t)|}\right)$, $\phi_{13} = \frac{180}{\pi}\cos^{-1}\left(\frac{u_{N_m}(t) \cdot w_{N_m}(t)}{|u_{N_m}(t)||w_{N_m}(t)|}\right)$. For a pure eigen mode, the phase difference between the transmissions for each pair of chains is $\phi_{12}^{E_2} = \phi_{23}^{E_2} = \pi/2$ and $\phi_{13}^{E_2} = \pi$ for E_2 and $\phi_{12}^{E_3} = \phi_{23}^{E_3} = \pi$ and $\phi_{13}^{E_3} = 0$ for E_3. From Fig. 5, we indeed see that manipulation of the parameter μ can be used to tune the eigen mode superposition, since for $\mu \neq 0$ and $\mu \neq 1$, the output mode is a linear combination of spatial eigen modes E_2, E_3 with corresponding k-labeled Bloch waves. In Fig. 5, we drive the system at different frequencies, between $\omega_D^{(c,d)} = 0.6$ that is in the vicinity of the two modes

c and d and $\omega_D^{(a,b)} = 0.622$ that is in the vicinity of the two modes a and b. In particular, for $\omega_D = 0.618$, we note that at $\mu = 0$, the spatial character across the planar array of waveguides that is measured is a pure E_2 state. For $0 < \mu < 0.2$, the measured spatial state is a superposition of modes E_2, E_3. At $\mu = 0.2$, the output mode is the well-defined superposition $(1 - 1 \ 0)$. For $\mu > 0.2$, the measured spatial output suggests a state very close to E_3 until $\mu = 1$, where the measured spatial character is purely E_3.

Figure 6 shows the variations of the phase difference as a function of the driving frequency ω_d and for different values of μ. We observe that some of the phase differences between pairs of waveguides change sign between the frequencies 0.6165 and 0.618. To shed light on these numerical results, we write an approximation to the amplitude of the displacement field, U_D, by considering only the contribution of the modes a, b, c, d within the first Brillouin zone,

$$U_D \sim \frac{F_2}{-\omega_D^2 + \omega_c^2 + i\eta\omega_D}E_2 e^{ik_2 QP} + \frac{F_2}{-\omega_D^2 + \omega_b^2 + i\eta\omega_D}E_2 e^{ik_3 QP}$$
$$+ \frac{F_3}{-\omega_D^2 + \omega_a^2 + i\eta\omega_D}E_3 e^{ik_2 QP} + \frac{F_3}{-\omega_D^2 + \omega_d^2 + i\eta\omega_D}E_3 e^{ik_3 QP}, \quad (38)$$

where the complex amplitudes resulting from the four modes are written as simple resonances with damping. $k_2 (= k_{a,c})$ is the wave number of modes a and c. The wave number $k_3 (= k_{b,d})$ corresponds to modes b and d.

We now consider a special case by choosing ω_D between ω_c and ω_d such that $-\omega_D^2 + \omega_c^2 = -\delta$ and $-\omega_D^2 + \omega_d^2 = \delta$. Note that δ is small. In that case, only two terms dominate. The approximate displacement field has now the components

$$U_{D,1} = C_1 e^{i\phi_1} = \frac{F_2}{-\delta + i\eta\omega_D}\frac{1}{\sqrt{2}}e^{ik_2 QP} + \frac{F_3}{\delta + i\eta\omega_D}\frac{1}{\sqrt{6}}e^{ik_3 QP}, \quad (39a)$$

$$U_{D,2} = C_2 e^{i\phi_2} = -\frac{F_2}{\delta + i\eta\omega_D}\frac{2}{\sqrt{6}}e^{ik_3 QP}, \quad (39b)$$

$$U_{D,3} = C_3 e^{i\phi_3} = \frac{F_2}{-\delta + i\eta\omega_D}\frac{-1}{\sqrt{2}}e^{ik_2 QP} + \frac{F_3}{\delta + i\eta\omega_D}\frac{1}{\sqrt{6}}e^{ik_3 QP}. \quad (39c)$$

When choosing another special case by driving the system at a frequency ω_D' that lies between ω_a and ω_b such that $-\omega_D'^2 + \omega_a^2 = -\delta$ and $-\omega_D'^2 + \omega_b^2 = \delta$, the components of the approximate field amplitude become

$$U_{D',1} = C_1' e^{i\phi_1'} = \frac{F_2}{\delta + i\eta\omega_D'}\frac{1}{\sqrt{2}}e^{ik_3 QP} + \frac{F_3}{-\delta + i\eta\omega_D'}\frac{1}{\sqrt{6}}e^{ik_2 QP}, \quad (40a)$$

$$U_{D',2} = C_2' e^{i\phi_2'} = \frac{F_3}{-\delta + i\eta\omega_D'}\frac{-2}{\sqrt{6}}e^{ik_2 QP}, \quad (40b)$$

$$U_{D',3} = C_3' e^{i\phi_3'} = \frac{F_2}{\delta + i\eta\omega_D'}\frac{-1}{\sqrt{2}}e^{ik_3 QP} + \frac{F_3}{-\delta + i\eta\omega_D'}\frac{1}{\sqrt{6}}e^{ik_2 QP}. \quad (40c)$$

The ratio of the amplitude measured at $x = QP$ along the first waveguide relative to that measured along the second waveguide is given by

$$\frac{U_{D,1}}{U_{D,2}} = G_1 e^{i\phi_{12}} = \frac{C_1}{C_2}e^{i\phi_{12}} = \frac{-\sqrt{3}}{2}\frac{F_2}{F_3}\frac{\delta + i\eta\omega_D}{-\delta + i\eta\omega_D}e^{i(k_2 - k_3)QP} - \frac{1}{2}, \quad (41)$$
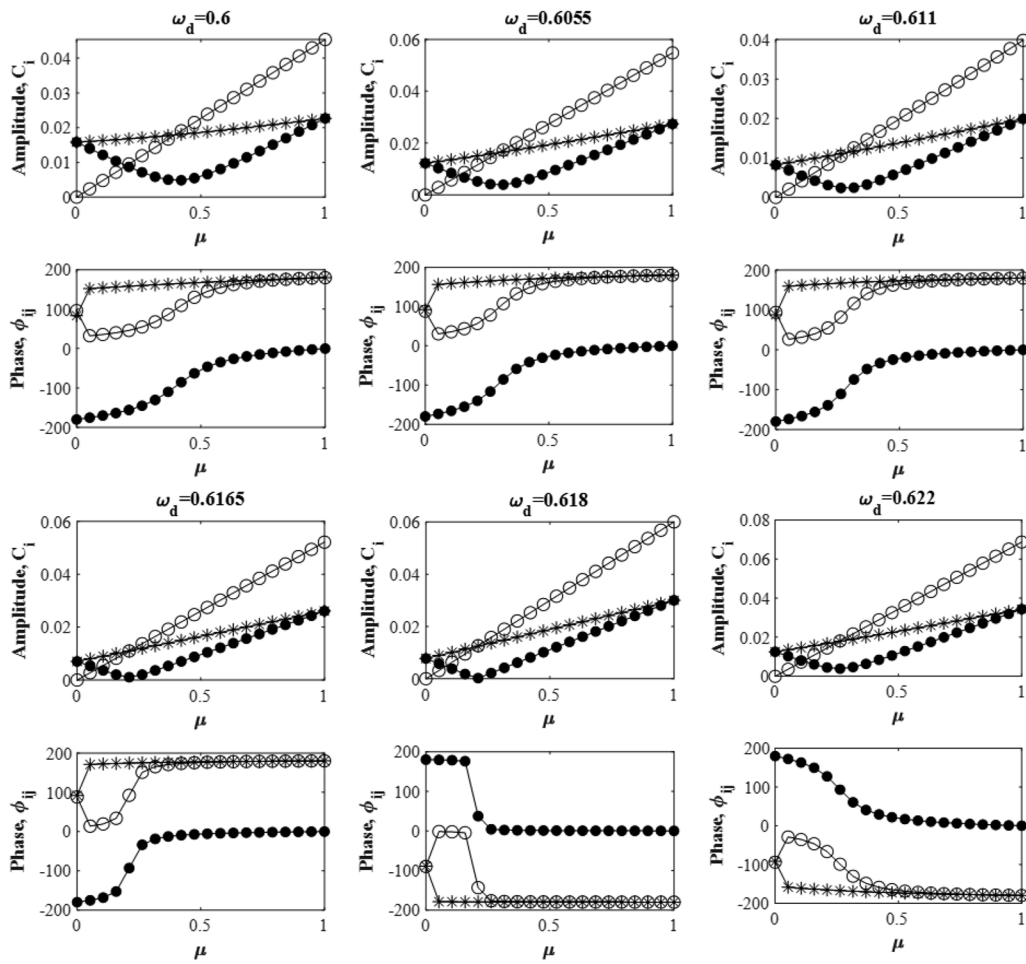
FIG. 5. Creation of nonseparable states by the external driving force $\vec{F}e^{i\omega_d t}$; $\vec{F} = (1 - \mu)E_2 + \mu E_3$, and driving frequency ω_D and variations of the maximum amplitudes of the last mass of each waveguide C_i; $C_1 = \max(u_{N_m}(t))$, $C_2 = \max(v_{N_m}(t))$, $C_3 = \max(w_{N_m}(t))$ (asterisks correspond to C_1, open circles correspond to C_2, and closed circles correspond to C_3) and phase differences (ϕ_{ij}) between pairs of chains (asterisks correspond to ϕ_{12}, open circles correspond to ϕ_{23}, and closed circles correspond to ϕ_{13}) of the coupled mass–spring waveguides as a function of μ. The phases are in degree. System parameters: $N_c = 204$, $\eta = 0.0114$, $(F_0^u, F_0^v, F_0^w) = (1, -2\mu, -1 + 2\mu)$, and $(\phi_0^u, \phi_0^v, \phi_0^w) = (0, 180 * \{-2\mu < 0\}, 180 * \{(-1 + 2\mu) < 0\})$.

FIG. 6. Variations of the phase differences (ϕ_{ij}) between pairs of chains (asterisks correspond to ϕ_{12}, open circles correspond to ϕ_{23}, and closed circles correspond to ϕ_{13}) of the coupled mass–spring waveguides as a function of the driving frequency ω_d and for different values of μ. The phases are in degree. System parameters: $N_c = 204$, $\eta = 0.0114$, $(F_0^u, F_0^v, F_0^w) = (1, -2\mu, -1 + 2\mu)$, and $(\phi_0^u, \phi_0^v, \phi_0^w) = (0, 180 * \{-2\mu < 0\}, 180 * \{(-1 + 2\mu) < 0\})$.
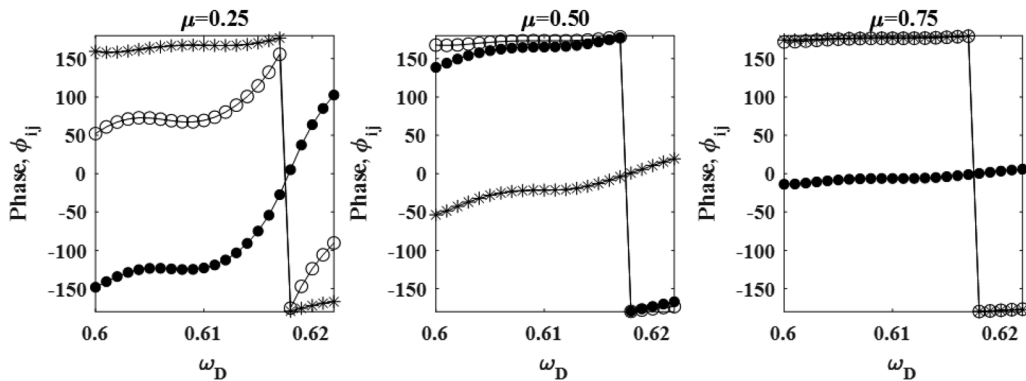
where the phase difference $\phi_{12} = \phi_1 - \phi_2$.

The ratio of amplitudes between waveguides 1 and 2 for the driving frequency ω'_D is obtained as

$$\frac{U_{D',1}}{U_{D',2}} = G'_1 e^{i\phi'_{12}} = \frac{C'_1}{C'_2} e^{i\phi'_{12}} = -\frac{1}{2} + \frac{-\sqrt{3}}{2} \frac{F_2}{F_3} \frac{-\delta + i\eta\omega'_D}{\delta + i\eta\omega'_D} e^{i(k_3 - k_2)QP},$$
(42)

with $\phi'_{12} = \phi'_1 - \phi'_2$.

Since the frequencies of the modes a, b, c, d are within a few percent of each other, the driving frequencies ω_D and ω'_D necessary to transform the displacement field from U_D to $U_{D'}$ are also within a few percent of each other. Therefore, Eq. (42) approximates the complex conjugate of Eq. (41). Subsequently, one has $\phi'_{12} \sim -\phi_{12}$. This is what is observed in Fig. 6. This observation can also be made for the ratios $\frac{U_{D,3}}{U_{D,2}} = \frac{C_3}{C_2} e^{i\phi_{32}}$ and $\frac{U_{D',3}}{U_{D',2}} = \frac{C'_3}{C'_2} e^{i\phi'_{32}}$, that is, $\phi'_{32} \sim -\phi_{32}$ that automatically applies to ϕ_{23}. However, with these simple cases, the approximate complex conjugation may not be true for ϕ_{13} in light of Eqs. (40a) and (40c). We recall that for a given set of driving parameters F_2 and F_3, i.e., for a given value of μ, raising of the driving frequency from ω_D to ω'_D executes the matrix operation of Eq. (30) on the displacement field amplitudes expressed in the $H_{E,k}$ basis. Complex conjugation is the signature of this operation in the space of the complex amplitudes of individual waveguides $\left(C_1 e^{i\phi_1}, C_2 e^{i\phi_2}, C_3 e^{i\phi_3}\right)$ or of the complex amplitudes relative to the first waveguide $\left(G_1, G_2 e^{i\phi_{12}}, G_3 e^{i\phi_{13}}\right)$.

To quantify the level of control the model allows, on the extent of the Hilbert space that can be explored, we calculate the coefficients in the transformation matrix of Eq. (30). For the sake of completeness, we rewrite Eq. (28) by including mode E_1, although we anticipate its contribution to be negligible in light of the way the system is stimulated. At the driving frequencies $\omega_D = 0.6$ and $\omega_{D'} = 0.622$, we get

$$U_D(QP,t) = \left(A_{1,1}E_1 e^{ik_1 x} + A_{2,2}E_2 e^{ik_2 x} + A_{3,3}E_3 e^{ik_3 x}\right)e^{i\omega_D t},$$
(43)

$$U_{D'}(QP,t) = \left(A_{1,1}E_1 e^{ik_1 x} + A_{2,3}E_2 e^{ik_3 x} + A_{3,2}E_3 e^{ik_2 x}\right)e^{i\omega_{D'} t}.$$
(44)

In writing Eqs. (43) and (44), we have used the fact that at the end of each waveguide, i.e., at $x = QP = N_c$ where the measurements are performed, $e^{igx} = 1$. Furthermore, in the mass–spring system with periodic boundary conditions, the wave numbers are integer multiples of $2\pi/N_c$, and hence, $e^{ik_1 x} = e^{ik_2 x} = e^{ik_3 x} = 1$. Simplifying the equations above, we obtain

$$\begin{pmatrix} G_1 \\ G_2 e^{i\phi_{12}} \\ G_3 e^{-i\phi_{13}} \end{pmatrix} e^{i\omega_D t} = \left[A_{1,1} \frac{1}{\sqrt{3}} \begin{pmatrix} 1 \\ 1 \\ 1 \end{pmatrix} + A_{2,2} \frac{1}{\sqrt{2}} \begin{pmatrix} 1 \\ 0 \\ -1 \end{pmatrix} \right.$$
$$\left. + A_{3,3} \frac{1}{\sqrt{6}} \begin{pmatrix} 1 \\ -2 \\ 1 \end{pmatrix} \right] e^{i\omega_D t},$$
(45)

$$\begin{pmatrix} G'_1 \\ G'_2 e^{i\phi_{12}} \\ G'_3 e^{i\phi_{13}} \end{pmatrix} e^{i\omega_{D'} t} = \left[A_{1,1} \frac{1}{\sqrt{3}} \begin{pmatrix} 1 \\ 1 \\ 1 \end{pmatrix} + A_{2,3} \frac{1}{\sqrt{2}} \begin{pmatrix} 1 \\ 0 \\ -1 \end{pmatrix} \right.$$
$$\left. + A_{3,2} \frac{1}{\sqrt{6}} \begin{pmatrix} 1 \\ -2 \\ 1 \end{pmatrix} \right] e^{i\omega_{D'} t}.$$
(46)

The measured amplitudes as a function of the driving parameter μ on the left of Eqs. (45) and (46) are used to calculate the complex coefficients $A_{1,1}, A_{2,2}, A_{3,3}, A_{2,3}$, and $A_{3,2}$ [as shown in Fig. 7(a)]. We find, as anticipated, that $A_{1,1}$ [shown by an asterisk in Fig. 7(a)] is zero. With the frequency ω_D and for $\mu = 0$, $A_{3,3} = 0$ and the spatial state is a pure mode E_2. For $\mu = 1$, the spatial state is a pure mode E_3 with $A_{2,2} = 0$. Similarly, with the frequency $\omega_{D'}$ and for $\mu = 0$, $A_{3,2} = 0$ and the spatial state is also a pure mode E_2. For $\mu = 1$, the spatial state is a pure mode E_3 with $A_{2,3} = 0$. Following Ref. 30,
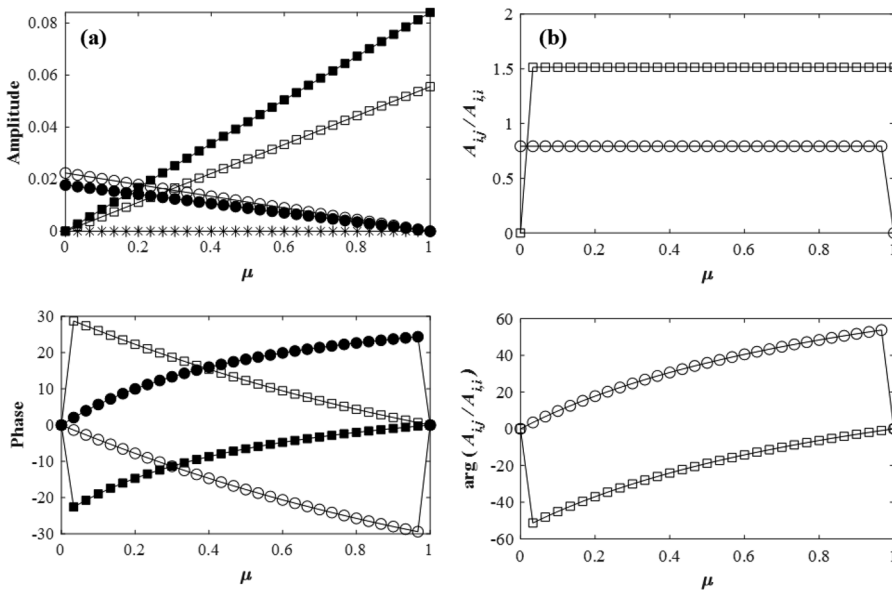

FIG. 7. Dependency on μ of the (a) complex amplitudes $A_{1,1}, A_{2,2}, A_{2,3}, A_{3,3}, A_{3,2}$ (asterisks: $A_{1,1}$, open circles: $A_{2,2}$, closed circles: $A_{2,3}$, open squares: $A_{3,3}$, closed squares: $A_{3,2}$) reported as modulus and phase and (b) modulus and phase of the ratios of non-zero off-diagonal terms $A_{i,j}/A_{i,i}; i, j = 2 : 3; i \neq j$ (open circles: $A_{2,3}/A_{2,2}$, open squares: $A_{3,2}/A_{3,3}$) of the transformation matrix of Eq. (30). The driving frequencies are $\omega_D = 0.6$ and $\omega_{D'} = 0.622$. The phases are in degree. System parameters: $N_c = 204, \eta = 0.0114, (F_0^u, F_0^v, F_0^w) = (1, -2\mu, -1 + 2\mu)$, and $\left(\phi_0^u, \phi_0^v, \phi_0^w\right) = (0, 180 * \{-2\mu < 0\}, 180 * \{(-1 + 2\mu) < 0\})$.

we can express the entropy of "entanglement" for the two driving frequencies

$$S = -\frac{1}{|A_{2,2}|^2 + |A_{3,3}|^2}\left(A_{2,2}A_{2,2}^*\ln\frac{A_{2,2}A_{2,2}^*}{|A_{2,2}|^2 + |A_{3,3}|^2}\right.$$
$$\left. + A_{3,3}A_{3,3}^*\ln\frac{A_{3,3}A_{3,3}^*}{|A_{2,2}|^2 + |A_{3,3}|^2}\right), \tag{47}$$

$$S' = -\frac{1}{|A_{2,3}|^2 + |A_{3,2}|^2}\left(A_{2,3}A_{2,3}^*\ln\frac{A_{2,3}A_{2,3}^*}{|A_{2,3}|^2 + |A_{3,2}|^2}\right.$$
$$\left. + A_{3,2}A_{3,2}^*\ln\frac{A_{3,2}A_{3,2}^*}{|A_{2,3}|^2 + |A_{3,2}|^2}\right). \tag{48}$$

We note that when $|A_{2,2}| = |A_{3,3}|$, $S = \ln 2$. The superposition of states is maximally "entangled." Maximum entanglement is also achieved for the driving frequency $\omega_{D'}$ when $|A_{2,3}| = |A_{3,2}|$, and $S' = \ln 2$.

We can calculate the ratios of complex amplitude coefficients, $A_{2,3}/A_{2,2}$ and $A_{3,2}/A_{3,3}$, constituting the off-diagonal terms in the non-trivial transformation matrix (quantum-like gate) of Eq. (30). The modulus and the corresponding phase of these ratios are reported in Fig. 7(b). The moduli remain constant for all values of μ. However, from Fig. 7(b), it is clear that we can navigate the phases between 0 and $3\pi/10$. Therefore, we have liberty to manipulate the drivers such that one can tune the block transformation matrix between the two nonseparable states of Eqs. (43) and (44). For instance, when $\mu \to 0$, the first block of the transformation matrix becomes proportional to the Pauli X matrix: $\begin{pmatrix} 0 & A_{2,3}/A_{2,2} \\ A_{2,3}/A_{2,2} & 0 \end{pmatrix} \propto \begin{pmatrix} 0 & 1 \\ 1 & 0 \end{pmatrix}$, while the second block is proportional to the nontrivial matrix: $\begin{pmatrix} 0 & A_{3,2}/A_{3,3} \\ A_{3,2}/A_{3,3} & 0 \end{pmatrix} \propto \begin{pmatrix} 0 & \cos 3\pi/10 + i\sin 3\pi/10 \\ \cos 3\pi/10 + i\sin 3\pi/10 & 0 \end{pmatrix}$.

Finally, we remark that the case discussed above is only one possible example of manipulation of states within the Hilbert space of product states and exploration of that space can be enlarged by choosing other input parameters for the drivers such as changing the relative phase of the drivers.

VII. CONCLUSIONS

A planar array of three one-dimensional elastic waveguides mutually coupled periodically along their length can be driven externally to support nonseparable superpositions of states. These states are the product of Bloch waves characterizing the elastic displacement along the waveguides and spatial modes representing the displacement across the array of waveguides. For a system composed of finite length waveguides, the frequency of external drivers can be employed to excite specific discrete modes. The periodicity induced band folding realizes superpositions of states that span the complete available Hilbert space of product states. By tuning the frequency and the relative amplitudes of the external drivers stimulating individual waveguides, we can navigate a broad segment of the Hilbert space of product states. Transformation from one type of nonseparable superposition to another one in the product

Hilbert space is analogous to a generalized Pauli gate. This transformation can also be interpreted as the complex conjugation operator in the space of the complex amplitudes of individual waveguides. Using similar elastic waveguides, although not periodic, we demonstrated Hadamard gate operations on the coherent superposition analogous to the single qubit gate operation in quantum computing.[17]

Finally, nonseparable or "classically entangled" states of elastic waves offer the advantage of stability over entangled states of true quantum systems. Nonseparable superpositions of elastic waves are robust against decoherence and will not require operating at cryogenic temperatures to maintain the delicate balance of the superpositions. Nonseparable superpositions of elastic waves do not suffer from the phenomenon of wave function collapse upon measurement. A coherent superposition of quantum states collapses into a pure state upon measurement. Multiple statistical measurements are, therefore, necessary to obtain information on the original superposition. Moreover, the present demonstration of (a) "classically entangled" superposition of elastic states that span their complete Hilbert space and (b) a transformation from one type of nonseparable superposition to another one analogous to a nontrivial quantum gate is a significant step toward realizing the potential of elastic waves in capturing quantum-like phenomena previously associated with optics. Recently, the use of classical light with entangled degrees of freedom has found applications in quantum information[33] and metrology.[34,35] The present study suggests that the same sort of applications can be realized with acoustic systems. The periodicity of the coupling between elastic waveguides was the determining factor for widening the Hilbert space accessible to elastic superposition of states. This coupling can be easily manipulated by choices of materials and fabrication. Moreover, due to the flexibility of the elastic system, the coupling can easily be tailored to be linear, periodic, and nonlinear (with different types or degrees of nonlinearity).[36,37]

AUTHORS' CONTRIBUTIONS

All authors contributed equally to this work.

ACKNOWLEDGMENTS

DATA AVAILABILITY

The data that support the findings of this study are available from the corresponding author upon reasonable request.

REFERENCES

[1] J. P. Dowling and G. J. Milburn, Philos. Trans. R. Soc., A **361**, 1655 (2003).
[2] R. J. C. Spreeuw, Found. Phys. **28**, 361 (1998).
[3] P. Ghose and A. Mukherjee, Rev. Theor. Sci. **2**, 274 (2014).
[4] E. Karimi and R. W. Boyd, Science **350**, 1172 (2015).
[5] E. Otte, I. Nape, C. Rosales-Guzmán, A. Vallés, C. Denz, and A. Forbes, Phys. Rev. A **98**, 053818 (2018).
[6] S. M. Hashemi Rafsanjani, M. Mirhosseini, O. S. Magaña-Loaiza, and R. W. Boyd, Phys. Rev. A **92**, 023827 (2015).
[7] L. J. Pereira, A. Z. Khoury, and K. Dechoum, Phys. Rev. A **90**, 053842 (2014).

[8] M. McLaren, T. Konrad, and A. Forbes, Phys. Rev. A **92**, 023833 (2015).

[9] P. Deymier and K. Runge, *Sound Topology, Duality, Coherence and Wave-Mixing: An Introduction to the Emerging New Science of Sound* (Springer International Publishing, 2017).

[10] Z. Zhang, Q. Wei, Y. Cheng, T. Zhang, D. Wu, and X. Liu, Phys. Rev. Lett. **118**, 084303 (2017).

[11] Z. Zhang, Y. Tian, Y. Cheng, X. Liu, and J. Christensen, Phys. Rev. B **96**, 241306 (2017).

[12] S.-Y. Yu, C. He, Z. Wang, F.-K. Liu, X.-C. Sun, Z. Li, H.-Z. Lu, M.-H. Lu, X.-P. Liu, and Y.-F. Chen, Nat. Commun. **9**, 3072 (2018).

[13] Y. Long, J. Ren, and H. Chen, Proc. Natl. Acad. Sci. U. S. A. **115**, 9951 (2018).

[14] P. A. Deymier, K. Runge, N. Swinteck, and K. Muralidharan, C. R. Mec. **343**, 700 (2015).

[15] P. A. Deymier, K. Runge, N. Swinteck, and K. Muralidharan, J. Appl. Phys. **115**, 163510 (2014).

[16] P. Deymier and K. Runge, Crystals **6**, 44 (2016).

[17] L. Calderin, M. A. Hasan, N. G. Jenkins, T. Lata, P. Lucas, K. Runge, and P. A. Deymier, Sci. Rep. **9**, 14156 (2019).

[18] D. Jia, H. Sun, J. Xia, S. Yuan, X. Liu, and C. Zhang, New J. Phys. **20**, 093027 (2018).

[19] J. Li, J. Wang, S. Wu, and J. Mei, AIP Adv. **7**, 125030 (2017).

[20] B.-G. Englert, K. L. Lee, A. Mann, and M. Revzen, J. Phys. A: Math. Gen. **39**, 1669 (2006).

[21] L. Wang, R.-Y. Zhang, M. Xiao, D. Han, C. T. Chan, and W. Wen, New J. Phys. **18**, 103029 (2016).

[22] R. K. Pal and M. Ruzzene, New J. Phys. **19**, 025001 (2017).

[23] M. A. Hasan, L. Calderin, P. Lucas, K. Runge, and P. A. Deymier, J. Sound Vib. **459**, 114843 (2019).

[24] M. A. Hasan, L. Calderin, P. Lucas, K. Runge, and P. A. Deymier, J. Acoust. Soc. Am. **146**, 748 (2019).

[25] H.-X. Wang, G.-Y. Guo, and J.-H. Jiang, New J. Phys. **21**, 093029 (2019).

[26] D. Zhang, J. Ren, T. Zhou, and B. Li, New J. Phys. **21**, 093033 (2019).

[27] Y. Meng, X. Wu, R.-Y. Zhang, X. Li, P. Hu, L. Ge, Y. Huang, H. Xiang, D. Han, S. Wang, and W. Wen, New J. Phys. **20**, 073032 (2018).

[28] J. Vila, R. K. Pal, M. Ruzzene, and G. Trainiti, J. Sound Vib. **406**, 363 (2017).

[29] P. A. Deymier and K. Runge, AIP Adv. **7**, 045020 (2017).

[30] M. A. Hasan, L. Calderin, T. Lata, P. Lucas, K. Runge, and P. A. Deymier, Commun. Phys. **2**, 106 (2019).

[31] M. A. Hasan, L. Calderin, T. Lata, P. Lucas, K. Runge, and P. A. Deymier, Appl. Sci. **10**, 3202 (2020).

[32] M. A. Hasan, L. Calderin, T. Lata, P. Lucas, K. Runge, and P. A. Deymier, Appl. Phys. Lett. **116**, 164104 (2020).

[33] C. Gabriel, A. Aiello, W. Zhong, T. G. Euser, N. Y. Joly, P. Banzer, M. Förtsch, D. Elser, U. L. Andersen, Ch. Marquardt, P. St, J. Russell, and G. Leuchs, Phys. Rev. Lett. **106**, 060502 (2011).

[34] F. Töppel, A. Aiello, C. Marquardt, E. Giacobino, and G. Leuchs, New J. Phys. **16**, 073019 (2014).

[35] B. N. Simon, S. Simon, F. Gori, M. Santarsiero, R. Borghi, N. Mukunda, and R. Simon, Phys. Rev. Lett. **104**, 023901 (2010).

[36] Q. Chen and A. Elbanna, Sci. Rep. **7**, 16204 (2017).

[37] T. Hikihara, Y. Okamoto, and Y. Ueda, Chaos **7**, 810 (1997).